

# Gas Accretion Traced in Absorption in Galaxy Spectroscopy

Kate H. R. Rubin

**Abstract** The positive velocity shift of absorption transitions tracing diffuse material observed in a galaxy spectrum is an unambiguous signature of gas flow toward the host system. Spectroscopy probing, e.g., Na I resonance lines in the rest-frame optical or Mg II and Fe II in the near-ultraviolet is in principle sensitive to the infall of cool material at temperatures  $T \sim 100 - 10,000$  K anywhere along the line of sight to a galaxy’s stellar component. However, secure detections of this redshifted absorption signature have proved challenging to obtain due to the ubiquity of cool gas outflows giving rise to blueshifted absorption along the same sightlines. In this chapter, we review the *bona fide* detections of this phenomenon. Analysis of Na I line profiles has revealed numerous instances of redshifted absorption observed toward early-type and/or AGN-host galaxies, while spectroscopy of Mg II and Fe II has provided evidence for ongoing gas accretion onto  $> 5\%$  of luminous, star-forming galaxies at  $z \sim 0.5 - 1$ . We then discuss the potentially ground-breaking benefits of future efforts to improve the spectral resolution of such studies, and to leverage spatially-resolved spectroscopy for new constraints on inflowing gas morphology.

## 1 Introduction

Spectroscopy of galaxy continua has been used for decades as a powerful probe of the kinematics of gas in the foreground. Absorption transitions sensitive to cool, diffuse material trace its motion with respect to the galaxy’s stellar component along the line of sight. The galaxy continuum “beam” is absorbed by gas over a broad range of scales, from the  $\sim 100 - 200$  pc scale heights of the dense interstellar medium (Langer et al., 2014) to the  $> 100$  kpc extent of the diffuse gas reservoir

---

Kate H. R. Rubin  
San Diego State University, Department of Astronomy, San Diego, CA 92182 e-mail:  
krubin@sdsu.edu

filling the galaxy halo (Prochaska et al., 2011; Tumlinson et al., 2011; Werk et al., 2014) and beyond.

The detection of absorption lines in a galaxy’s spectrum (i.e., “down the barrel”) which are *redshifted* with respect to its rest frame is unequivocal evidence of gas flow toward the continuum source. And while this signature arises from material at any location along the sightline to the galaxy, such that the flow may not ultimately reach the galaxy itself, redshifted absorption has been broadly interpreted as strong evidence for gas inflow toward or accretion onto the background host. Over the past ten years, as high signal-to-noise (S/N) galaxy spectroscopy covering the rest-frame optical into the near-ultraviolet has become more routine, this technique has become sensitive to the inflow of material over a broad range of densities and temperatures: redshifted Ca II H & K  $\lambda\lambda 3934, 3969$  or Na I D  $\lambda\lambda 5891, 5897$  absorption probes cold, mostly neutral gas infall at a temperature  $T < 1000$  K; redshifts in low-ionization transitions such as Mg II  $\lambda\lambda 2796, 2803$  or Fe II  $\lambda\lambda 2586, 2600$  trace the inflow of cool, photoionized gas at  $T \sim 10^4$  K; and the detection of redshifted C IV  $\lambda\lambda 1548, 1550$  or Si IV  $\lambda\lambda 1394, 1402$  absorption would in principle trace yet warmer ( $T \sim 10^5$  K) gas accretion.

Furthermore, unlike background QSO absorption line experiments, which typically must adopt the assumption that inflowing gas has a relatively low metallicity ( $Z/Z_\odot < 1$ ; Lehner et al., 2013) in order to disentangle accreting systems from those enriched by galactic outflows, redshifted self-absorption naturally traces metal-rich inflow, and may even trace pristine inflow in rare cases where spectral coverage of Ly $\alpha$  is available (Fathivavsari et al., 2016). Moreover, while studies searching for the signature of gas accretion in emission from the 21cm transition of neutral hydrogen are currently limited by the faint surface brightness of such features to galaxies within a few hundred Mpc of our own (Martin et al., 2010), the “down the barrel” technique has been used to detect gas accretion onto galaxies as distant as  $z \sim 1$  (Coil et al., 2011; Rubin et al., 2012; Martin et al., 2012).

In spite of these clear advantages, however, the first report of redshifted absorption observed down the barrel toward a sample of more than a single object did not occur until 2009 (Sato et al., 2009). Even today, secure detections of this phenomenon have been reported for only  $\sim 60 - 80$  systems. Instead, measurements of *blueshifted* absorption tracing cool gas outflow have dominated the literature (Heckman et al., 2000; Martin, 2005; Rupke et al., 2005b; Weiner et al., 2009; Steidel et al., 2010; Chen et al., 2010b). Large-scale galactic winds, thought to be driven by processes associated with star formation, are now known to arise ubiquitously in star-forming objects from the local universe to  $z > 2$  (Heckman et al., 2000; Ajiki et al., 2002; Martin et al., 2012; Rubin et al., 2014). These winds are likewise traced by all of the metal-line absorption features listed above, and are observed to have velocities ranging from  $\sim -50$  km s $^{-1}$  to  $< -800$  km s $^{-1}$  (Steidel et al., 2010; Rubin et al., 2014; Du et al., 2016). As the free-fall velocity of material within the virial radius of a typical massive, star-forming galaxy halo at  $z \sim 0$  (with halo mass  $M_h \sim 10^{11-12} M_\odot$ ) is expected to be only  $\sim 100 - 200$  km s $^{-1}$  (Goerdt & Ceverino, 2015), the preponderance of winds covering the sightlines to galaxies must necessarily obscure the detection of material falling inward at such comparatively modest

velocities. Indeed, this issue is compounded by the low spectral resolution of the vast majority of spectroscopic surveys useful for these analyses (Weiner et al., 2009; Steidel et al., 2010; Martin et al., 2012; Rubin et al., 2014).

In this chapter, we review the works in which the few *bona fide* instances of gas inflow were reported, beginning with the first detections via transitions in the rest-frame optical in Section 2. Due to technical limitations (described below), the focus of these early studies was on red, early-type galaxies and/or galaxies exhibiting signs of AGN activity. Reports of inflow onto galaxies hosting the most luminous AGN (i.e., bright QSOs) are discussed in Section 2.3. In Section 3, we describe the first detections of inflow onto actively star-forming systems facilitated by high-S/N spectroscopic galaxy surveys in the rest-frame ultraviolet. The biases inherent in the use of the “down the barrel” technique given the ubiquity of galactic winds are described in Section 4.1, and unique constraints on the morphology of gas inflow which will soon be facilitated by ongoing spatially-resolved spectroscopic surveys are discussed in Section 4.2. Section 5 presents a summary, and offers some recommendations for future experiments which will leverage the full potential of this technique in the detection and characterization of the process of gas accretion onto galaxies.

## 2 First Detections: Gas Accretion in Late-Stage Galaxy Evolution

For galaxy spectroscopy to successfully constrain the kinematics of absorption lines along the line of sight, it must have sufficient continuum S/N in the spectral range surrounding the transition in question. The limiting S/N depends in detail on a number of factors, including the typical equivalent width of the transition and the complexity of the absorption line analysis employed. Studies testing this limit and adopting a simple, “single component” analysis have required between  $S/N \sim 5 \text{ \AA}^{-1}$  (for analysis of Mg II; Rubin et al., 2014) and  $S/N \sim 15 \text{ \AA}^{-1}$  (for analysis of Na I D; Sato et al., 2009).

Many of the first works to attempt constraints on the kinematics of such absorption transitions *in galaxies not specifically selected to be starbursts* – i.e., in magnitude-limited galaxy samples representative of “typical” star-forming or quiescent objects – used datasets which did not broadly satisfy these S/N requirements (Weiner et al., 2009; Rubin et al., 2010; Chen et al., 2010b; Steidel et al., 2010). Each of these studies were leveraging spectroscopic samples obtained for the primary purpose of conducting a redshift survey, rather than an assessment of cool gas kinematics. As a result, these works often resorted to co-adding subsamples of tens or hundreds of spectra to achieve the S/N required for absorption line analysis. Moreover, this co-added spectroscopy yielded absorption profiles which were universally asymmetric with excess equivalent width blueward of the galaxies’ rest frame. The first detections of redshifted absorption profiles were reported only in later studies which obtained high-S/N spectroscopy of *individual* galaxies.

## 2.1 First Reports of Inflow Observed Down the Barrel

The very first detections of redshifted self-absorption made use of some of the highest-S/N spectroscopy obtained during the execution of the DEEP2 redshift survey (Davis et al., 2003). In their discussion of a massive ultraluminous infrared galaxy with an X-ray-bright central AGN at  $z = 1.15$  located in the AEGIS survey field (Davis et al., 2007), Le Floch et al. (2007) commented on strong Ca II H & K absorption lines which were redshifted by  $\sim 150 - 200 \text{ km s}^{-1}$  relative to the velocity of [O II] emission from the host.

Shortly thereafter, Sato et al. (2009) significantly expanded the sample of redshifted self-absorption detections through their analysis of Na I D kinematics in a S/N-limited subsample of the DEEP2 survey of the Extended Groth Strip. The parent DEEP2 sample was magnitude-selected to  $R < 24.1$ , such that it contained substantial populations of both star-forming and passive galaxies. However, Sato et al. (2009) found that they required at least  $S/N \sim 6.5 \text{ pix}^{-1}$  in the rest-frame continuum around Na I D to constrain its velocity to within a 68% confidence interval spanning less than  $\sim 200 \text{ km s}^{-1}$ . This limited their analysis sample to 205 objects at  $0.11 < z < 0.54$ , about 75% of which are “red sequence” galaxies. Outflows and inflows are reported in this work if the fitted Na I centroid is shifted from systemic velocity by more than  $\pm 50 \text{ km s}^{-1}$ , and occur in nearly equal numbers: outflows are detected in 32 objects, while inflows are detected with high confidence in 31 objects.

The Na I profiles shown in the left-hand panel of Fig. 1 demonstrate the typical quality of the data used in this analysis. As the two transitions in the Na I D doublet are separated by only  $\sim 300 \text{ km s}^{-1}$ , the lines are blended in these spectra due to the large intrinsic velocity of both the stellar and gas components giving rise to the observed absorption. The velocity  $v(\text{Na I D}) = 0 \text{ km s}^{-1}$  on the x-axis corresponds to the rest wavelength of the  $5897 \text{ \AA}$  doublet transition. The authors show their best-fit absorption line model for each spectrum with colored curves, and mark the corresponding best-fit velocity of the  $\lambda 5897 \text{ \AA}$  transition with vertical dotted lines. The top-most spectrum exhibits significantly redshifted absorption with a fitted velocity of  $\sim +80 \text{ km s}^{-1}$ .

Sato et al. (2009) note that while a significant fraction of the galaxies in their sample which exhibit outflows are star-forming and lie in the so-called “blue cloud” (blue symbols; Fig. 1, right), all but one of the objects exhibiting inflows occupy the red sequence (red symbols; Fig. 1, right). In interpreting this finding, they caution that there may be additional absorption features arising from the stellar populations in these systems which are not yet understood, and which could in principle shift the minimum of the stellar continuum flux near  $\lambda_{\text{obs}} \sim 5890 - 5900 \text{ \AA}$  redward of the rest wavelengths of Na I D. Line-profile fitting of such features could in turn be mistakenly interpreted as redshifted interstellar absorption. However, the authors also report that many of the inflow galaxies in their sample exhibit optical emission line ratios ( $[\text{N II}]/\text{H}\alpha$ ) consistent with Seyfert or LINER activity, and draw an intriguing comparison to the inflows observed in neutral hydrogen in the inner re-

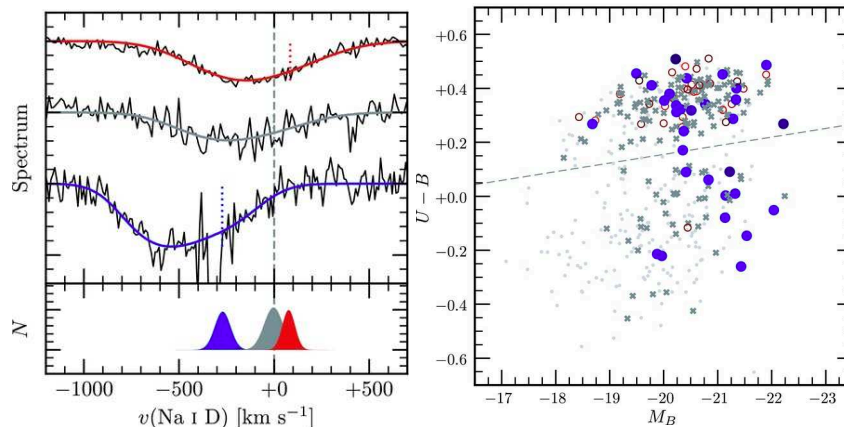


**Fig. 1 Spectroscopy and photometry of the sample analyzed in Sato et al. (2009), the first study to report and characterize gas accretion onto distant galaxies.** *Left:* Continuum-normalized spectra showing the region around the Na I doublet (black).  $v = 0 \text{ km s}^{-1}$  is set at the systemic velocity of the  $\lambda 5897$  doublet transition. The colored curves show the best-fit absorption line models, and the vertical dotted lines show the corresponding best-fit velocity of the  $\lambda 5897$  line. The bottom panel shows the marginalized probability distributions of the model profile velocity for each spectrum, obtained from a Markov Chain Monte Carlo sampling of the absorption line profile parameters. *Right:* Rest-frame color-magnitude diagram showing the full sample. Objects exhibiting outflows are marked with blue filled circles; those exhibiting redshifted absorption are marked with red open circles; and gray crosses mark objects which exhibit neither significant blueshifts nor redshifts in their Na I profiles. The light gray dots indicate objects whose spectra lack the S/N required to constrain their absorption line kinematics. The dashed line divides the blue cloud and red sequence populations. Panels are reproductions of Figures 4 (left) and 10 (right) from the article “AEGIS: The Nature of the Host Galaxies of Low-Ionization Outflows at  $z < 0.6$ ”, by T. Sato et al. (2009, ApJ, 696, 214). ©AAS. Reproduced with permission.

gions of radio-bright elliptical galaxies (van Gorkom et al., 1989). They speculate that the observed absorbing gas may in fact feed this central activity.

## 2.2 Inflows onto AGN-Host Galaxies

Since the publication of this novel and important work, there have been several studies corroborating the detection of inflow toward galaxies hosting active AGN. Krug et al. (2010) explored Na I D kinematics in a sample of Seyfert galaxies selected to be infrared-faint (with  $10^{9.9} < L_{\text{IR}}/L_{\odot} < 10^{11}$ ). Previous studies of Na I D absorption toward nearby galaxy samples had targeted infrared-bright starburst or starburst/AGN composite systems (Rupke et al., 2005b,a; Martin, 2005), and had detected outflows in the majority of these objects. A primary goal of Krug et al. (2010) was to develop a comparison sample of objects without ongoing starbursts to determine the relative contributions of star formation vs. AGN activity in driving these winds. The authors obtained spectroscopy of 35 galaxies using the RC

Spectrograph on the Kitt Peak 4m telescope. With a median S/N near Na I D of  $\sim 85 \text{ \AA}^{-1}$  and a spectral resolution of  $85 \text{ km s}^{-1}$ , they performed both single- and double-velocity component absorption line model fits with typical central velocity uncertainties of  $< 50 \text{ km s}^{-1}$ .

In contrast to previous studies of starbursting systems, Krug et al. (2010) detected outflows traced by Na I in only 4 galaxies (11% of their sample) and instead detected inflows in over a third (13 galaxies) of their sample. The central velocities of these flows ranged from just over  $+50 \text{ km s}^{-1}$  to  $+140 \text{ km s}^{-1}$ ; however, no significant correlation between inflow kinematics and host galaxy mass, infrared luminosity, or inclination was observed. From this analysis, the authors concluded that star formation rather than AGN activity makes the dominant contribution to the driving of outflows (although this conclusion does not apply to Type 1 Seyferts; Krug et al., 2010). Furthermore, they speculated that the high observed inflow velocities are suggestive of material located close to the galaxy nuclei rather than in the outskirts of the disks. They also searched for signs of nuclear morphological features which could indicate that the inflowing material is undergoing angular momentum loss, finding that 5 galaxies in their inflow sample exhibit nuclear dust spirals, bars, or rings. Five additional inflow galaxies have nearby companions with which they may be interacting. Such phenomena are thought to be required in order to facilitate the inflow of gas toward galaxy nuclei and its ultimate accretion onto the central black hole.

The high quality of these data also permitted a rough estimate of the rate of mass inflow onto these systems via constraints on the Na I column density. Assuming a factor of 10 ionization correction (i.e., that  $N(\text{Na})/N(\text{Na I}) = 10$ ), a metallicity approximately twice the solar metallicity, and that the absorbing gas is at a distance of  $r = 1 \text{ kpc}$  from the nucleus, it is estimated to be flowing inward at  $(1 - 5) \frac{r}{1 \text{ kpc}} M_{\odot} \text{ yr}^{-1}$ . This rate is approximately two orders of magnitude larger than the mass accretion rate required to power a typical Seyfert nucleus (Crenshaw et al., 2003; Krug et al., 2010). These cold gas inflows may therefore serve as an important fueling mechanism for AGN activity in these objects.

Yet further evidence for massive inflows of gas onto AGN-host galaxies was reported by Stone et al. (2016), who studied molecular gas kinematics in a sample of 52 local AGN selected from the *Swift*-Burst Alert Telescope Survey of hard X-ray objects. The Stone et al. (2016) targets thoroughly sample the AGN luminosity function to its brightest end. The authors analyzed spectroscopy of these systems covering the OH  $119 \mu\text{m}$  feature obtained with the *Herschel*/PACS far-IR interferometer, detecting the transition in absorption in 17 sources. As in the Krug et al. (2010) study discussed above, only a handful (four) of these 17 AGN exhibited molecular outflows, while the OH absorption feature was redshifted by  $> 50 \text{ km s}^{-1}$  in seven of their targets (corresponding to a detection rate of  $\sim 40\%$ ). The authors suggested that the significantly lower detection rates of inflows toward IR-luminous galaxies may be due to the disruption of these accretion flows by the faster winds driven by their central starbursts.

### 2.3 Inflows on the Smallest Scales: Feeding Luminous QSOs?

Spectroscopy of bright quasars also probes gas flows toward the central source (i.e., the AGN), and can be obtained with much greater efficiency than faint galaxy spectroscopy. Indeed, the SDSS-I/II and SDSS-III BOSS redshift surveys have now revealed several instances of redshifted absorption observed toward bright QSOs (Hall et al., 2002, 2013). These profiles occur in quasars with “broad” absorption lines (BAL), defined to extend over thousands of  $\text{km s}^{-1}$  in velocity (Allen et al., 2011). In addition, the absorption typically only partially covers the emitting source. The vast majority of BAL QSOs exhibit absorption troughs lying entirely at velocities blueward of systemic, and are thought to arise from AGN-driven feedback/outflow. However, in their search through more than 100,000 SDSS/BOSS QSO spectra, Hall et al. (2013) discovered 19 BAL objects in which the trough in at least one transition extends to velocities  $v > 3000 \text{ km s}^{-1}$ . These authors estimated that such redshifts occur in approximately 1 in every 1000 BAL quasars.

This work discusses several different physical scenarios which may explain the observed extreme absorption. The accretion of material onto the host dark matter halo or host galaxy at kpc-scale distances from the central source may certainly contribute to the redshifted absorption signal; however, the free fall velocity of such material is expected to be only a few hundred  $\text{km s}^{-1}$ . For gas to achieve an infall velocity  $v > 3000 \text{ km s}^{-1}$ , it must reach scales as small as a few hundred Schwarzschild radii (Hall et al., 2013). It remains to be established whether infalling gas clumps can maintain sufficiently high densities at such small distances to give rise to absorption in the observed transitions (e.g., Si IV, C IV, Al III  $\lambda\lambda$  1854, 1862, Mg II). Hydrodynamical simulations of accretion flows onto a supermassive black hole may be used to address this question; e.g., Li et al. (2013); however, detailed predictions of absorption profile shapes in multiple transitions are needed for a quantitative comparison to the observations. Alternative scenarios which could give rise to redshifted, broad absorption include gravitational redshifting of a spherically symmetric wind; rotating accretion disk winds observed toward an extended emission source; outflow from a *second* QSO close in the foreground to the first; or even the relativistic Doppler effect of outflowing ions absorbing photons of lower frequency due to time dilation. Hall et al. (2013) concluded that none of these mechanisms can individually explain the observations; however, they suggest that both rotationally-dominated accretion disk winds and infalling material are likely contributing to the redshifted broad absorption profiles.

In some instances, these data may also constrain the distance between the absorbing material and the central black hole. Shi et al. (2016) analyzed one of the BAL QSOs discussed in Hall et al. (2013), reporting the detection not only of redshifted Mg II and Fe II line profiles but also redshifted hydrogen Balmer and He I\*  $\lambda$ 3889 absorption. The latter transition is highly sensitive to the number of ionizing photons impinging on the gas per ion ( $U$ ), while Balmer absorption lines generally arise only in very high-density environments ( $n(\text{H}) > 10^6 \text{ cm}^{-3}$ ; Shi et al., 2016). Together with an estimate of the ionizing luminosity of the QSO, constraints on both  $U$  and  $n(\text{H})$  from analysis of the He I\* and Balmer lines imply a distance of  $r_{\text{abs}} \sim 4$

pc for this particular absorbing system. Shi et al. (2016) note that this distance is much larger than expected for a rotating disk wind or a gravitationally redshifted AGN outflow, and suggest that it is instead consistent with infall from the inner surface of a dusty torus surrounding the accretion disk (Barvainis, 1987). Detailed analysis of a larger sample of similar systems has the potential to more conclusively establish the frequency of such infall events, the mass of material involved, and their overall contribution to the fueling of bright QSOs.

Apart from the BAL phenomenon, QSOs are observed to exhibit numerous other classes of foreground absorbers. One such class – that of ‘proximate’ absorbers – differs from BALs primarily in that they have significantly more narrow velocity widths ( $< 100 \text{ km s}^{-1}$ ). Proximate absorbers are typically defined to have a central velocity within  $< 10,000 \text{ km s}^{-1}$  of the QSO emission line redshift, and are often (though not always) observed to fully cover the emitting source (Ellison et al., 2010). Recently, Fathivavsari et al. (2016) presented a sample of six  $z \sim 2$  QSOs in which a proximate damped Ly $\alpha$  (DLA) absorber entirely eclipses the broad Ly $\alpha$  emission from the central AGN. They report that in five of these systems, the absorber has a velocity  $\sim 100 - 1200 \text{ km s}^{-1}$  redward of the QSO systemic velocity, speculating that the absorption traces infalling material. However, because this work relies on spectroscopy of broad QSO emission lines to constrain the host galaxy redshift (e.g., C IV, C III]  $\lambda 1909$ , He II  $\lambda 1640$ ), these estimates suffer from significant systematic uncertainties ( $\sim 200 - 500 \text{ km s}^{-1}$ ; Shen et al., 2016). Followup spectroscopy covering [O II]  $\lambda 3728$  or [O III]  $\lambda 5007$  in the near-infrared will be important for verifying this intriguing finding.

## 2.4 Inflows onto Early-Type and Post-Starburst Galaxies

Concomitant with the assembly of this compelling evidence for gas accretion onto active AGN, two studies offered additional empirical support for inflow onto red sequence galaxies, or galaxies exhibiting signs of recent quenching. In the first study to obtain rest-frame near-UV galaxy spectroscopy of sufficient depth for analysis of Fe II  $\lambda\lambda 2586, 2600$  and Mg II  $\lambda\lambda 2796, 2803$  absorption in individual sightlines, Coil et al. (2011) targeted a sample of 10 X-ray-luminous AGN and 13 post-starburst galaxies at  $0.2 < z < 0.8$  selected from the DEEP2 and SDSS redshift surveys. The AGN are moderately luminous, with  $\log(L_X/\text{erg s}^{-1}) \sim 41 - 42$ , while the post-starbursts were identified via a decomposition of their optical spectroscopy into old and young stellar population components. Those objects for which spectral fitting yielded a relatively luminous young component (contributing at least 25% of the continuum at  $\lambda_{\text{rest}} \sim 4500 \text{ \AA}$ ) and which exhibited little or no H $\beta$  emission were targeted. The Keck/LRIS spectroscopy obtained for this study traced blueshifted absorption in 60% of the AGN and 31% of the post-starbursts, but also yielded redshifted absorption profiles in two of the latter. These redshifts were detected in Mg II (and in one case in Mg I  $\lambda 2852$ ) at speeds of  $75 - 115 \text{ km s}^{-1}$ , but were not detected securely in Fe II absorption. While it is difficult to draw definitive conclusions from

such small sample sizes, the ubiquitous detection of Mg II and Fe II absorption in excess of that predicted for the stellar continuum in these spectra suggests that the mechanism causing the cessation of star formation did not completely deplete the gas supply in these systems.

Most recently, Sarzi et al. (2016) undertook a study of Na I absorption in SDSS spectra of galaxies selected to have high-spatial-resolution 20cm continuum coverage obtained with the Very Long Baseline Array (Deller et al., 2014). Nearly 60% of this sample are early-type galaxies, and the vast majority of these early types do not exhibit blueshifted Na I. The authors briefly comment on their detection of redshifted absorption in  $\sim 10 - 20$  objects, most of which either exhibit very weak optical emission lines or LINER/Seyfert-like emission line ratios. It is suggested that this phenomenon may be the signature of bars or unsettled dust lanes in these systems.

## 2.5 Summary

In summary, cool gas kinematics have now been assessed in relatively small samples of early-type and/or AGN-host galaxies. Measurements of Na I absorption velocities toward red sequence systems suggest a  $\sim 20\%$  incidence rate of redshifted profiles (Sato et al., 2009). Spectroscopy of Seyfert galaxies and X-ray-selected AGN reveals a yet higher incidence ( $\sim 40\%$ ) of redshifted Na I or OH absorption (Krug et al., 2010; Stone et al., 2016). These rates are approximately the same or higher than the outflow detection rates for the same samples:  $\sim 14\%$  for the red sequence sample of Sato et al. (2009) and  $\sim 10 - 25\%$  for the Seyfert and BAT/AGN samples of Krug et al. (2010) and Stone et al. (2016). While the mass of these flows remains poorly constrained, the similar rates of these phenomena may ultimately point to a “steady state” of gas cycling through such systems (even as they maintain very low rates of star formation).

It should also be noted, however, that the physical scale over which these flows occur may in fact be limited to the regions very close to or within the galaxies’ stellar component. The common use of Na I in the aforementioned studies naturally biases these assessments to tracing the motions of cold, dust-enshrouded material, which in red-sequence galaxies may in fact lie in dust lanes or cold molecular disks (Sato et al., 2009; Davis et al., 2011). Spectroscopy of additional transitions tracing gas over a broader range of density and temperature (e.g., Mg II or Fe II) will be important for developing constraints on the physical state and scale of these flows.

### 3 Tracing Inflows with Rest-Frame Ultraviolet Galaxy Spectroscopy

As discussed above, the initial focus in the literature on Na I absorption kinematics biased these samples toward the highest surface-brightness systems at  $\lambda_{\text{rest}} \sim 5900 \text{ \AA}$  – i.e., infrared-selected starbursts, massive ellipticals, and bright AGN hosts. It was not until large surveys obtaining deep, high-S/N spectroscopy in the rest-frame ultraviolet were performed that the first constraints on cool gas kinematics toward a significant ( $> 50$ ) sample of individual, “normal” *star-forming* galaxies were discussed. Moreover, the Mg II and Fe II absorption transitions covered in these spectra can be significantly stronger than Na I due to a number of factors; e.g., Mg and Fe are more abundant than Na, and their singly-ionized transitions trace a much broader range of temperature and density than neutral Na. UV galaxy spectra therefore have the potential to trace more diffuse material, including the halo gas which is known to give rise to Mg II absorption in background QSO sightlines to projected distances of  $R_{\perp} \sim 100 \text{ kpc}$  (Bergeron, 1986; Steidel et al., 1994; Kacprzak et al., 2007; Chen et al., 2010a). Rest-frame UV transitions are thus significantly more sensitive to both inflow and outflow, and are accessible at observed-frame optical wavelengths for galaxies at  $z > 0.3$ .

The first unambiguous detection of inflow observed down the barrel toward a sample of star-forming galaxies was reported in Rubin et al. (2012). The galaxies were targeted over the course of a high-S/N Keck/LRIS survey of  $\sim 100$  galaxies at redshifts  $0.3 < z < 1.4$  (Rubin et al., 2014). This sample, selected to a magnitude limit  $B_{\text{AB}} < 23$ , spans the star-forming sequence at  $z \sim 0.5$ , and is thus representative of the “normal” star-forming galaxy population (Fig. 2, left). In addition, this survey targeted fields with deep *HST*/ACS imaging, facilitating a detailed morphological analysis (Fig. 2, right).

Blueshifted absorption tracing outflows was detected in the majority ( $\sim 66\%$ ) of this sample. Moreover, the detection rate of these winds does not vary significantly with the star formation rate (SFR) or stellar mass of the host, but rather depends primarily on galaxy orientation (Fig. 2, right). This finding is suggestive not only of ubiquitous outflows, but also of an approximately biconical morphology for these flows across the star-forming sequence.

In the same survey, redshifted absorption tracing cool inflow was detected in six of the remaining galaxy spectra (red diamonds in Fig. 2; Fig. 3) with velocities  $\sim 80 - 200 \text{ km s}^{-1}$ . The galaxies themselves have SFRs ranging from  $\sim 1 - 40 M_{\odot} \text{ yr}^{-1}$ , and have stellar masses in the range  $9.6 < \log M_{*}/M_{\odot} < 10.5$ . Perhaps most significantly, five of these six galaxies have disk-like morphologies and are viewed in a nearly edge-on orientation (with inclinations  $> 55^{\circ}$ ; Fig. 2, right). The authors suggest that the preferential detection of inflows toward edge-on galaxies indicates that cool infall is more likely to occur along the plane of galactic disks, rather than along the minor axis. We also note here that higher sensitivity to inflows in more edge-on systems is a natural consequence of biconical winds.

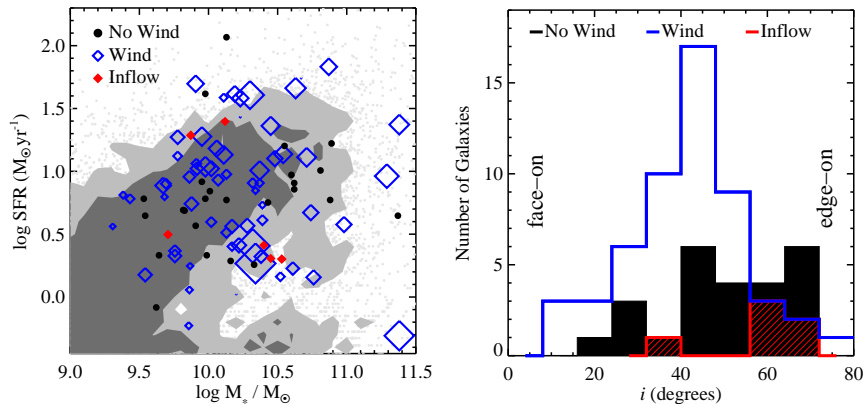


**Fig. 2** The first survey to detect cool gas inflow traced by Mg II and Fe II absorption onto a sample of distant star-forming galaxies (Rubin et al., 2012, 2014). *Left*: Colored and black points show the sample of  $\sim 100$  galaxies targeted in Rubin et al. (2012, 2014), and gray contours show the SFR- $M_*$  distribution of the underlying galaxy population (Barro et al., 2011). Blue open diamonds indicate galaxies with detected winds, red filled diamonds mark objects with inflows, and black circles indicate objects with neither winds nor inflow. The size of the blue diamonds is scaled with the Mg II equivalent width of the outflow. Winds are detected in  $\sim 2/3$  of the galaxies, while detected inflows occur at a rate  $\sim 6\%$ . *Right*: Distribution of inclinations ( $i$ ) for the disk-like galaxies selected from the same study. The distribution for galaxies with winds is shown in blue, and the distributions for galaxies with inflows and without winds/inflows are shown in red and black, respectively. While face-on galaxies (at low  $i$ ) are significantly more likely to drive a detected wind than galaxies viewed edge-on, the galaxies with detected inflow are nearly all highly inclined. Panels are adapted from Rubin et al. (2012, 2014).

Assuming a metallicity for these flows of  $Z = 0.1Z_\odot$  and adopting constraints on the inflow Mg II and Fe II column densities from their absorption line analysis, Rubin et al. (2012) estimated lower limits for the mass accretion rates onto this sample of six objects in the range  $\sim 0.2 - 3 M_\odot \text{yr}^{-1}$ . These observed flow rates are approximately consistent with the rate of mass flow onto our own Galaxy (Lehner & Howk, 2011).

Nearly concurrently, Martin et al. (2012) carried out a similar but completely independent study of cool gas kinematics in Keck/LRIS spectroscopy of  $\sim 200$  galaxies. The galaxy sample has a somewhat higher median redshift than that of Rubin et al. (2012) ( $\langle z \rangle \sim 0.5$  vs.  $\sim 1$ ) and is selected to a fainter magnitude limit  $B_{\text{AB}} < 24.0$ . However, the vast majority of the targets are star-forming, with SFRs ranging from  $\sim 1 - 98 M_\odot \text{yr}^{-1}$  and stellar masses  $8.85 < \log M_* / M_\odot < 11.3$ . This survey made use of a somewhat lower-resolution spectroscopic setup for  $\sim 70\%$  of the sample (having a FWHM resolution element  $\sim 435 \text{ km s}^{-1}$  vs.  $\sim 282 \text{ km s}^{-1}$ ), which in principle limits sensitivity to lower-velocity flows. In spite of this, redshifted absorption profiles were detected in nine spectra (see Fig. 4), yielding a detection rate ( $\sim 4\%$ ) consistent with that of Rubin et al. (2012). Martin et al. (2012) also performed a careful analysis of the two-dimensional spectra of these objects,

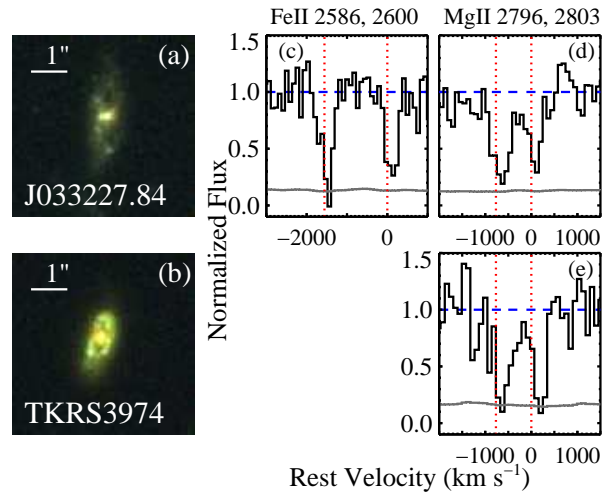


**Fig. 3** Imaging and spectroscopy of two galaxies with ongoing gas inflow. The left column shows *HST/ACS* images, and the middle and right columns show Fe II and Mg II transitions in the galaxy spectra. The line profiles are redshifted with respect to systemic velocity (marked with vertical dotted lines). Analysis of the imaging indicates that these galaxies are disk-like with edge-on orientations. The figure is a reproduction of a portion of Figure 1 from the article “The Direct Detection of Cool, Metal-Enriched Gas Accretion onto Galaxies at  $z \sim 0.5$ ”, by K. H. R. Rubin et al. (2012, *ApJL*, 747, 26). ©AAS. Reproduced with permission.

identifying weak nebular line emission offset from the continuum trace at the same velocity as the redshifted absorption in a few (4) cases. They speculated that the inflows in these systems are being fed by relatively dense, star-forming structures (e.g., satellite dwarf galaxies) rather than diffuse accretion streams from the circumgalactic medium.

Martin et al. (2012) found that the galaxies exhibiting inflows span the range in stellar mass and SFR occupied by the parent sample. They also noted that among the four inflow galaxies for which quantitative morphologies are available, only one has a high inclination ( $i \sim 61^\circ$ ); the remaining three galaxies have  $i < 55^\circ$  (Kornei et al., 2012). The detection of inflow toward these objects requires that the idea put forth by Rubin et al. (2012) that infall is more likely to be observed along the plane of galactic disks be considered more carefully and investigated with a significantly larger spectroscopic sample.

These two studies have provided us with the first, unequivocal evidence for gas accretion onto distant, star-forming galaxies. However, the physical nature of these flows remains an open question. There are numerous potential sources for the enriched material producing the observed absorption, including gas which has been tidally stripped from nearby dwarf galaxies, or wind ejecta from the central galaxy which is being recycled back to the disk. Indeed, such wind recycling is predicted in numerous cosmological galaxy formation simulations (Oppenheimer et al., 2010;

Vogelsberger et al., 2013). Current absorption line data cannot distinguish between these alternatives; however, detailed constraints on the covering fraction or cross section of the inflow from upcoming integral field spectroscopic surveys may aid in differentiating between these scenarios. This topic will be discussed further in Sections 4.2 and 5.

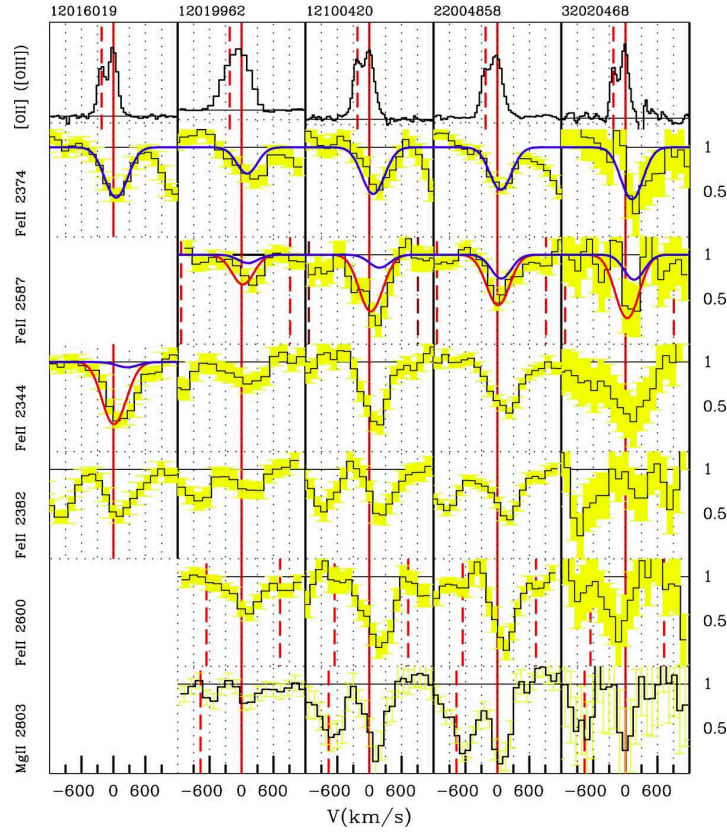


**Fig. 4** Resonant absorption lines and [O II] emission profiles for five galaxies with securely-detected inflows from Martin et al. (2012). Galaxy ID numbers are indicated at the top of each column. The solid red vertical lines mark the rest-frame velocity of each transition, and dashed vertical lines mark the wavelengths of nearby resonant transitions. Single-component absorption line fits are shown in the row of Fe II  $\lambda 2374$  profiles, and fits including both an absorption component with a velocity fixed at  $0 \text{ km s}^{-1}$  and a “flow” component are overplotted on the Fe II  $\lambda 2586$  profiles. These objects exhibit strong redshifts in most of the absorption transitions shown. The [O II] profiles are used to determine the systemic velocity. This figure is a reproduction of Figure 16 from the article “Demographics and Physical Properties of Gas Outflows/Inflows at  $0.4 < z < 1.4$ ”, by C. L. Martin et al. (2012, ApJ, 760, 127). ©AAS. Reproduced with permission.

## 4 Toward Assessment of the Incidence of Inflow

Ultimately, empirical studies characterizing the cool gas flows around galaxies must constrain, e.g., the incidence of accretion in a given galaxy population as a function of the mass inflow rate and age of the universe. Such detailed assessments are required for an incisive test of galaxy formation models (Davé et al., 2012; Nelson et al., 2015). We now consider a few factors which complicate the use of current datasets in developing such constraints. In the following section we discuss future directions which may ameliorate these issues.

### 4.1 Spectral Confusion

The faintness of the galaxies studied in Rubin et al. (2012) and Martin et al. (2012) forced the selection of a low resolution spectroscopic setup for these surveys (FWHM  $\sim 250 - 400 \text{ km s}^{-1}$ ). Thus, the velocity profiles arising from distinct inflowing and outflowing gas structures along the same line of sight are blended in these spectra. Indeed, in none of the Mg II or Fe II line profiles discussed in Rubin et al. (2014) is more than one velocity component resolved. If there is, e.g., a component of gas being accreted at  $v \sim +100 \text{ km s}^{-1}$ , and another wind component foreground to the same galaxy beam moving at  $v \sim -200 \text{ km s}^{-1}$ , a centroid of the resulting line profile (observed at low resolution) will suggest the presence of an outflow with a velocity  $v \sim -100 \text{ km s}^{-1}$  (while the inflowing component is completely obscured). Or, in the case of two components each at  $v \sim +100 \text{ km s}^{-1}$  and  $-100 \text{ km s}^{-1}$ , a centroid of the observed line profile will reveal neither outflow nor inflow. Thus, there is a limited set of circumstances in which the centroid of such blended profiles will be significantly redshifted, revealing an inflow.

Indeed, as noted in Rubin et al. (2012), the six objects toward which inflows were detected are unique not for the material moving at positive velocities along the line of sight, but for the *absence of winds*. This is demonstrated in Fig. 5, which compares the equivalent widths measured redward and blueward of systemic velocity in the Fe II  $\lambda 2600$  (left) and Mg II  $\lambda 2803$  (right) transitions in the spectral sample of Rubin et al. (2014). Objects with detected winds are marked with blue crosses and cyan triangles; objects with detected inflows are marked with red crosses; and objects with neither winds nor inflow are marked with black filled circles. A 1:1 relation is indicated with the dashed lines. Inflows were detected in galaxies with larger red EWs than blue EWs; however, there are many other systems which have red EWs larger than the smallest values measured for the inflow sample (i.e., red  $\text{EW}_{2600} > 0.6 \text{ \AA}$  and red  $\text{EW}_{2803} > 0.8 \text{ \AA}$ ; see Fig. 5). Based on an accounting of the number of galaxies with red EWs at least as large as those in which inflow was detected, Rubin et al. (2012) estimated that inflow must be occurring in at least 20-40% of the full galaxy sample.

Sensitivity to inflow in the presence of absorption due to winds or interstellar material is certainly improved at higher spectral resolution. The Na I spectroscopy

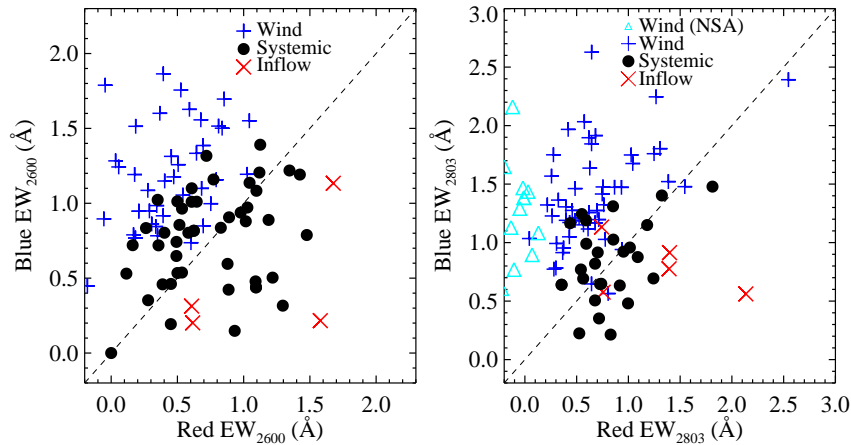
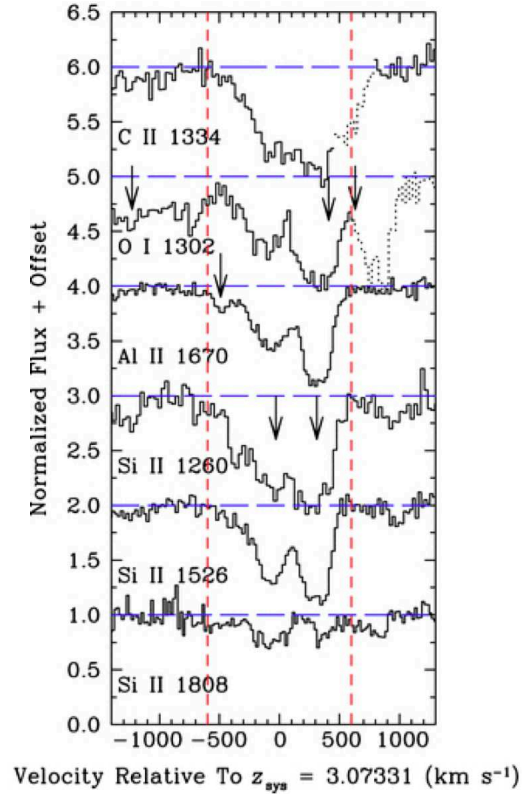


**Fig. 5** Assessment of the symmetry of Fe II and Mg II absorption line profiles in low-resolution galaxy spectroscopy. All measurements shown are from analysis of the UV spectroscopy of  $\sim 100$  star-forming galaxies discussed in Rubin et al. (2012, 2014). *Left*: The equivalent width (EW) of the Fe II  $\lambda 2600$  transition, measured at  $v < 0 \text{ km s}^{-1}$  (“blue”), vs. the EW of the same transition at  $v > 0 \text{ km s}^{-1}$  (“red”) for galaxies with blueshifted Fe II (blue crosses), without winds or inflows (black filled circles), and with inflows detected in Fe II (red crosses). Several galaxies without detected inflows have red  $\text{EW}_{2600}$  values  $> 0.6 \text{ \AA}$ , comparable to or larger than the red  $\text{EW}_{2600}$  for two of the inflow galaxies. *Right*: same as left-hand panel, for the Mg II  $\lambda 2803$  transition. Spectra which have no detectable absorption at  $v > 0 \text{ km s}^{-1}$  are marked with cyan triangles. As is the case for Fe II  $\lambda 2600$ , numerous galaxies without detected inflows have red  $\text{EW}_{2803} > 0.8 \text{ \AA}$ , the smallest value measured for the inflow sample. This survey is therefore likely failing to flag ongoing inflow in a significant fraction of those galaxies in the “wind” and “systemic” subsamples. This Figure is a reproduction of Figure 7 from the article “Evidence for Ubiquitous Collimated Galactic-Scale Outflows Along the Star-Forming Sequence at  $z \sim 0.5$ ”, by K. H. R. Rubin et al. (2014, ApJ, 794, 156). ©AAS. Reproduced with permission.

of nearby Seyfert galaxies discussed in Krug et al. (2010) (see Section 2.2) has a FWHM velocity resolution of  $\sim 85 \text{ km s}^{-1}$ , and is thus significantly more sensitive to detailed line profile shapes than that of Rubin et al. (2012) or Martin et al. (2012). Such high spectral resolution can be achieved with current technology for distant galaxies which are also strongly gravitationally lensed (e.g. Pettini et al., 2002; Quider et al., 2009, 2010; Dessauges-Zavadsky et al., 2010). If at  $z > 2$ , high-resolution optical spectroscopy of these targets offers the added advantage of coverage of a rich suite of rest-frame UV transitions, including Ly $\alpha$ , O I  $\lambda 1302$ , several Si II transitions, Si IV  $\lambda\lambda 1393, 1402$ , and C IV  $\lambda\lambda 1548, 1550$ .

Keck/ESI coverage of many of these transitions in a spectrum of the “Cosmic Eye” is shown in Fig. 6, adapted from Quider et al. (2010). The Cosmic Eye is a Lyman break galaxy (LBG) at  $z = 3.073$  which is heavily magnified by foreground massive structures, producing two overlapping arcs on the sky. The Keck/ESI spectroscopy obtained by Quider et al. (2010) has a FWHM velocity resolution

**Fig. 6 High resolution Keck/ESI spectrum showing rest-frame UV absorption lines in a lensed Lyman break galaxy at  $z_{\text{sys}} = 3.073$**  published in Quider et al. (2010). Arrows mark absorbers unrelated to this system. The values on the x-axis indicate velocity relative to  $z_{\text{sys}}$ . The absorption transitions shown trace either cool, photoionized material (e.g., C II, Al II, Si II) or neutral gas (O I) along the sightline. The spectrum resolves two absorbing “components”, one at  $v \sim -70 \text{ km s}^{-1}$  and one at  $v \sim +350 \text{ km s}^{-1}$ , suggesting both ongoing outflow and accretion. Spectroscopy of similar quality and fidelity of a significantly larger galaxy sample will reveal the frequency with which these phenomena occur along the same line of sight. This Figure reproduces a portion of Figure 4 from the article “A study of interstellar gas and stars in the gravitationally lensed galaxy ‘the Cosmic Eye’ from rest-frame ultraviolet spectroscopy” by A. M. Quider et al. (2010, MNRAS, 402, 1467). Reproduced with the permission of Oxford University Press.



$\sim 75 \text{ km s}^{-1}$ , and successfully resolves at least two distinct absorption components in several transitions. In fact, the authors note that this spectrum exhibits a strong, redshifted absorption component with  $v \sim 350 \text{ km s}^{-1}$  in addition to a blueshifted component presumably arising from winds. This may be interpreted as yet another detection of gas accretion, the first at  $z \sim 3$ . Indeed, the red absorption component in this line profile was unique among the lensed LBGs that had been studied to date, each of which exhibited strongly (and exclusively) blueshifted absorption.

Moreover, these data may in principle be used to constrain the column density, metallicity, and mass of the absorbing gas to a substantially higher level of precision than is possible with spectroscopy covering only the Na I or Mg II and Fe II lines. The absorption in the latter two transitions is nearly always saturated, limiting the line-

of-sight column density to be larger than a modest value (e.g.,  $N_{\text{MgII}} \sim 10^{14} \text{ cm}^{-2}$  or  $N_{\text{H}} \sim 10^{18.4} \text{ cm}^{-2}$  assuming solar metallicity; Rubin et al., 2012; Martin et al., 2012). Furthermore, rest-frame optical and near-UV spectroscopy cannot be used to measure the column density of hydrogen toward the galaxy, nor does it cover transitions of a given element in multiple levels of ionization for constraints on the ionization state of the material. While the S/N of the spectrum of the Cosmic Eye discussed above is insufficient for such analysis, spectroscopy of other lensed LBGs, e.g. the “Cosmic Horseshoe” (Quider et al., 2009), MS1512-cB58 (Pettini et al., 2002), and the “8 o’clock arc” (Dessauges-Zavadsky et al., 2010) has yielded ionic column density measurements for ISM and outflow absorbing components to a precision of  $\pm 0.1$  dex via analysis of weak (and unsaturated) Si II and Fe II transitions. Combined with analysis of the Ly $\alpha$  line profiles in the same spectra, this work has offered some of the only constraints on the metallicity of gas known to be outflowing from distant galaxies. Deeper observations of the Cosmic Eye and expanded samples of high dispersion, rest-frame far-UV spectroscopy of lensed LBGs have the potential to yield important constraints on the mass and metallicity of both outflows and cool galactic gas accretion.

## 4.2 Spatial Resolution

In addition to increasing spectral resolution to gain sensitivity to gas accretion, spatially resolving the background stellar beams will further improve our constraints on the morphology of inflow. Westmoquette et al. (2013) offered one of the earliest demonstrations of the potential of this technique, targeting the central regions of the M82 starburst with four pointings of the DensePak IFU on the WIYN telescope (Fig. 7). These observations achieved 3-arcsec spatial resolution at a spectral resolution of  $\sim 45 \text{ km s}^{-1}$ . Combined with CO emission observations from Walter et al. (2002), they facilitated a detailed comparison between the kinematics of H $\alpha$  emission, CO emission, and Na I absorption.

The authors extracted spectra from a pseudo-slit 7 arcseconds in width placed along the major axis of the system, co-adding the data in several spatial bins along the slit. Measurements of the H $\alpha$ , Na I, and CO velocities in these bins are shown in the right-hand panel of Fig. 7. In general, these velocities are similar at all slit locations; however, there is one component of Na I absorption (green) which has a large velocity offset, appearing to counter-rotate. The authors suggest that this component could be due to infalling tidal debris, which may even have originated in the HI gas filaments populating the circumgalactic medium around this system.

While this interpretation is somewhat speculative, this spatially resolved spectroscopy has nevertheless resolved a heretofore unknown velocity component of cold gas in a system in which gas flows have been studied in great detail for over a decade (Shopbell & Bland-Hawthorn, 1998). Moreover, these data provide evidence in support of a picture in which inflows persist even in strongly starbursting systems with powerful ongoing outflows. Upcoming massive IFU surveys such as

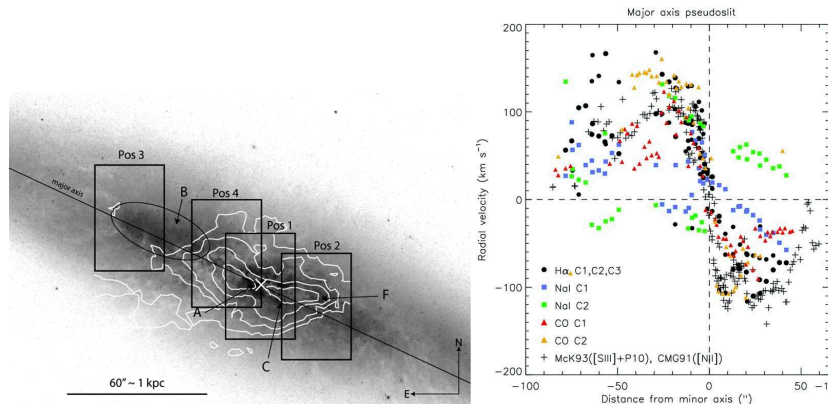


**Fig. 7 Spatially resolved spectroscopy of the starburst galaxy M82.** *Left:* *HST/ACS* image of M82 with four IFU pointings overlaid (rectangles). The white contours show the total CO flux from Walter et al. (2002). *Right:* Radial velocity of Na I, H $\alpha$ , and CO measured in a 7 arcsecond pseudo-slit extracted from the IFU data along the major axis. The CO and H $\alpha$  velocities are similar across the galaxy; however, there is an absorbing component of Na I (green) which is offset in velocity by many tens of km s $^{-1}$ . Westmoquette et al. (2013) suggest that this component may be due to accreting tidal debris. Panels are reproductions of Figures 1 (left) and 7 (right) from the article “Spatially resolved kinematics of the multi-phase interstellar medium in the inner disc of M82” by M. S. Westmoquette et al. (2013, MNRAS, 428, 1743). Reproduced with the permission of Oxford University Press.

SDSS-IV/MaNGA (Bundy et al., 2015) will provide qualitatively similar observations for  $\sim 10,000$  nearby galaxies, resolving Na I kinematics on  $\sim 1 - 2$  kpc spatial scales across the face of each object. These data will be extremely sensitive to the morphology and cross section of inflowing streams as they approach the ISM of galaxies.

## 5 Summary and Future Directions

Deep galaxy spectroscopy has now provided perhaps the only unequivocal evidence for the inflow of gas toward galaxies beyond the local universe. While the earliest spectroscopic datasets probing cool gas kinematics “down the barrel” specifically targeted starbursting galaxies and typically reported only blueshifted (i.e., outflowing) absorption (Heckman et al., 2000; Rupke et al., 2005b; Martin, 2005), later surveys achieving the requisite S/N have revealed numerous instances of redshifted metal-line absorption profiles toward a wide variety of host systems. Study of Na I D profiles in spectra of red-sequence galaxies at  $z \sim 0.3$  has suggested an incidence rate of inflow of  $\sim 20\%$ ; i.e., similar to the rate of outflow detections for the same sample (Sato et al., 2009). Spectroscopy of Na I and the OH  $119\mu\text{m}$  feature in the far-IR in small samples of nearby Seyfert and X-ray-bright AGN hosts points to a yet

higher rate of redshifted cool gas absorption ( $\sim 40\%$ ; Krug et al., 2010; Stone et al., 2016). Such inflows may in fact be necessary to fuel the observed nuclear activity; however, the amount of mass carried in these flows remains poorly constrained, and current observations do not establish the present (or ultimate) location of the gas along the line of sight (although see Shi et al., 2016, for an exception to this generalization).

In the few years following these first detections, deep spectroscopy of Fe II and Mg II transitions in the rest-frame near-UV has finally revealed evidence for inflow onto “normal” star-forming galaxies at  $z > 0.3$  (Rubin et al., 2012; Martin et al., 2012). The reported rate of incidence is low ( $< 10\%$ ), as blueshifted absorption tends to dominate the metal-line profiles in these spectra. Furthermore, Rubin et al. (2012) has presented evidence suggesting that inflow is more likely to be detected in these star-forming systems when they are viewed in an edge-on orientation. However, Martin et al. (2012) reported detections of inflow toward galaxies viewed over a wide range of orientations, and hence do not support this claimed dependence of inflow detection rate on viewing angle.

Such studies have been pivotal for furthering our understanding of the cycling of cool gas through galaxy environments. However, the evidence they offer is anecdotal rather than statistical. A complete, empirical picture of the baryon cycle must establish the incidence, mass, and morphology of gas inflow as a function of host galaxy stellar mass, star formation activity and history, and AGN luminosity. As all of the aforementioned samples are S/N-limited, they cannot assess such quantities regardless of their spectral resolution or the transitions they probe. Surveys of cool gas kinematics in samples selected to be complete to a given stellar mass limit (i.e., unbiased in their distributions of SFR and galaxy orientation) are required if we are to make substantive progress in our development of an empirical model of galactic gas flows.

At the same time, the observational challenges inherent in such an effort are significant. The works discussed in Section 3 surveying samples of  $\sim 100 - 200$  objects in the rest-frame near-UV together represent an investment of  $\sim 17$  nights on the Keck 1 Telescope (Rubin et al., 2012; Martin et al., 2012). A stellar mass-complete survey of a significantly larger sample would require a yet more extensive observing campaign. The ongoing SDSS-IV/MaNGA survey (Bundy et al., 2015) will facilitate a major advancement in our constraints on the incidence and morphology of inflow in the near term, as it will obtain high-S/N, spatially resolved spectroscopy of Na I in an unprecedented sample of  $\sim 10,000$  nearby galaxies. The MaNGA sample selection is carefully designed to be complete to a stellar mass  $\log M_*/M_\odot > 9$ , and its observing procedure ensures a minimum S/N per fiber of  $\sim 6$  per pix at 1.5 effective radii. Although its spectral coverage is limited to Ca II and Na I at relatively low velocity resolution ( $R \sim 2000$ ), its  $\sim 1 - 2$  kpc spatial resolution will enable detailed mapping of the incidence of cold, dusty gas inflow at speeds  $> 40 \text{ km s}^{-1}$  in an extremely large galaxy sample.

To assess the mass and metallicity of these flows, deep, high resolution rest-frame far-UV spectroscopy will be required (Quider et al., 2009, 2010; Dessauges-Zavadsky et al., 2010). Such observations of samples of more than a few objects must await the next

generation of wide-field multi-object spectrographs on 30m-class ground-based optical telescopes. As laid out in the Thirty Meter Telescope Detailed Science Case (Skidmore, 2015), the prospective instrument WFOS will be capable of obtaining  $R \sim 5000$  spectroscopy of more than 100 (unlensed) LBGs at  $z \sim 2 - 3$  with  $R_{AB} < 24.5$  simultaneously.  $S/N > 30$  will be achieved in just a few hours for these spectra, which will cover all of the ionic transitions discussed in the context of the Cosmic Eye (Section 4.1), including  $\text{Ly}\alpha$ , O I, several Si II transitions, several Fe II transitions, Al III, Si IV, and C IV. Such a dataset will permit detailed constraints on the column densities, ionization states, metallicities, and mass of gas components arising in the ISM, outflows, and in accreting streams at high redshift.

Similarly detailed characterization of gas flows at  $z < 1.5$  must await the next UV-sensitive space mission. A prospective high-resolution imaging spectrograph (France et al., 2016) conceived for the Large Ultraviolet/Optical/InfraRed (LUVOIR) surveyor NASA mission concept will not only access the important UV transitions discussed above, but will do so at a spatial resolution of  $\sim 10 - 100$  pc. This instrument will readily differentiate between material flowing inward in accreting streams from ongoing outflow and establish the mass and morphology of this accreting material. These capabilities will ultimately allow us to complete our empirical picture of the cycling of diffuse baryons through galaxy environments.

## References

- Ajiki, M., Taniguchi, Y., Murayama, T. et al. 2002, ApJ, 576, 25  
 Allen, J. T., Hewett, P. C., Maddox, N. et al. 2011, MNRAS, 410, 860  
 Barro, G., Pérez-González, P. G., Gallego, J. et al. 2011, ApJS, 193, 13  
 Barvainis, R. 1987, ApJ, 320, 537  
 Bergeron, J. 1986, A&A, 155, L8  
 Bundy, K., Bershady, M. A., Law, D. R. et al. 2015, ApJ, 798, 7  
 Chen, H.-W., Helsby, J. E., Gauthier J.-R., et al. 2010, ApJ, 714, 1521  
 Chen, Y.-M., Tremonti, C. A., Heckman, T. M. et al. 2010, AJ, 140, 445  
 Coil, A., Weiner, B. J., Holz, D. E., et al. 2011, ApJ, 743, 23  
 Crenshaw, D. M., Kraemer, S. B., George, I. M. 2003, ARA&A, 41, 117  
 Davé, R., Finlator, K., Oppenheimer, B. D. 2012, MNRAS, 421, 98  
 Davis, M., Faber, S. M., Newman, J. et al. 2003, SPIE, 4834, 161  
 Davis, M., Guhathakurta, P., Konidaris, N. P., et al. 2007, ApJ, 660, 1  
 Davis, T. A., Alatalo, K., Sarzi, M., et al. 2011, MNRAS, 417, 882  
 Deller, A. T., Middelberg, E. 2014, AJ, 147, 14  
 Dessauges-Zavadsky, M., D’Odorico, S., Schaerer, D. et al. 2010, A&A, 510, 26  
 Du, X., Shapley, A. E., Martin, C. L., Coil, A. L. 2016, arXiv, 1604.03945  
 Ellison, S. L., Prochaska, J. X., Hennawi, J. et al. 2010, MNRAS, 406, 1435  
 Fathivavari, H., Petitjean, P., Noterdaeme, P. et al. 2016, MNRAS, 461, 1816  
 France, K., Fleming, B., Hoadley, K. 2016, J. Astron. Telesc. Instrum. Syst., 2(4), 041203  
 Goerdt, T., Ceverino, D. 2015, MNRAS, 450, 3359  
 Hall, P. B., Anderson, S. F., Strauss, M. A. et al. 2002, ApJ, 141, 267  
 Hall, P. B., Brandt, W. N., Petitjean, P. et al. 2013, MNRAS, 434, 222  
 Heckman, T. M., Lehnert, M. D., Strickland, D. K., Armus, L. 2000, ApJS, 129, 493  
 Kacprzak, G. G., Churchill, C. W., Steidel, C. C. et al. 2007, ApJ, 662, 909

- Kornei, K. A., Shapley, A. E., Martin, C. L. et al. 2012, *ApJ*, 758, 135  
Krug, H. B., Rupke, D. S. N., Veilleux, S. 2010, *ApJ*, 708, 1145  
Langer, W. D., Pineda, J. L., Velusamy, T. 2014, *Astronomy & Astrophysics*, 564, 101  
Le Floch, E., Willmer, C. N. A., Noeske, K. et al. 2007, *ApJ*, 660, 65  
Lehner, N., Howk, J. C. 2011, *Science*, 334, 955  
Lehner, N., Howk, J. C., Tripp, T. M., et al. 2013, *ApJ*, 770, 138  
Li, J., Ostriker, J., Sunyaev, R. 2013, *ApJ*, 767, 105  
Martin, C. L. 2005, *ApJ*, 621, 227  
Martin, A. M., Papastergis, E., Giovanelli, R. et al. 2010, *ApJ*, 723, 1359  
Martin, C. L., Shapley, A. E., Coil, A. L. et al. 2012, *ApJ*, 760, 127  
Nelson, D., Genel, S., Vogelsberger, M. et al. 2015, *MNRAS*, 448, 59  
Oppenheimer, B. D., Dave, R., Kereš, D. et al. 2010, *MNRAS*, 406, 2325  
Pettini, M., Rix, S. A., Steidel, C. C., et al. 2002, *ApJ*, 569, 742  
Prochaska, J. X., Weiner, B. J., Chen, H.-W., et al. 2011, *ApJ*, 740, 91  
Quider, A. M., Pettini, M., Shapley, A. E., Steidel, C. C. 2009, *MNRAS*, 398, 1263  
Quider, A. M., Shapley, A. E., Pettini, M. et al. 2010, *MNRAS*, 402, 1467  
Rupke, D. S., Veilleux, S., Sanders, D. B. 2005b, *ApJS*, 160, 115  
Rupke, D. S., Veilleux, S., Sanders, D. B. 2005a, *ApJ*, 632, 751  
Rubin, K. H. R., Weiner, B. J., Koo, D. C., et al. 2010, *ApJ*, 719, 1503  
Rubin, K. H. R., Prochaska, J. X., Koo, D. C., Phillips, A. C., 2012, *ApJL*, 747, 26  
Rubin, K. H. R., Prochaska, J. X., Koo, D. C., et al. 2014, *ApJ*, 794, 156  
Sarzi, M., Kaviraj, S., Nedelchev, B., et al. 2016, *MNRAS*, 456, 25  
Sato, T., Martin, C. L., Noeske, K. G., et al. 2009, *ApJ*, 696, 214  
Shen, Y., Brandt, W. N., Denney, K. D., et al. 2016, *arXiv*, 1602.03894  
Shi, X., Jiang, P., Wang, H., et al. 2016, *arXiv*, 1608.05487  
Shopbell, P. L. & Bland-Hawthorn, J. 1998, *ApJ*, 493, 129  
Steidel, C. C., Dickinson, M., Persson, S. E. 1994, *ApJ*, 437, L75  
Steidel, C. C., Erb, D. K., Shapley, A. E., et al. 2010, *ApJ*, 717, 289  
Stone, M., Veilleux, S., Melendez, M. 2016, *arXiv*, 1605.06512  
Thirty Meter Telescope Detailed Science Case 2015, ed. Skidmore, W., *arXiv*:1505.01195  
Tumlinson, J., Thom, C., Werk, J. K. et al. 2011, *Science*, 334, 948  
van Gorkom, J. H., Knapp, G. R., Ekers, R. D., et al. 1989, *AJ*, 97, 708  
Vogelsberger, M., Genel, S., Sijacki, D., et al. 2013, *MNRAS*, 436, 3031  
Walter, F., Weiss, A., Scoville, N. 2002, *ApJ*, 580, 21  
Weiner, B. J., Coil, A. L., Prochaska, J. X., et al. 2009, *ApJ*, 692, 187  
Werk, J. K., Prochaska, J. X., Tumlinson, J., et al. 2014, *ApJ*, 792, 8  
Westmoquette, M. S., Smith, L. J., Gallagher, J. S., Walter, F. 2013, *MNRAS*, 428, 1743